An Optimal Bipolar MVDC Coaxial Power Cable Design for Envisaged All Electric Wide Body Aircraft

Anoy Saha, Arian Azizi, and Mona Ghassemi
Zero Emission, Realization of Optimized Energy Systems (ZEROES) Laboratory
Department of Electrical and Computer Engineering, The University of Texas at Dallas, Richardson, TX, USA
anoy.saha@utdallas.edu, arian.azizi@utdallas.edu, mona.ghassemi@utdallas.edu

2023 IEEE Conference on Electrical Insulation and Dielectric Phenomena (CEIDP) | 979-8-3503-3562-0/23/$31.00 ©2023 IEEE | DOI: 10.1109/CEIDP51414.2023.10410570

***Abstract*- Future generations of electrified aircraft, such as more electric aircraft (MEA) and all-electric aircraft (AEA), will require high-power-delivery and low-system-mass electric power systems (EPS). Designing aircraft cables confronts thermal challenges due to the limited heat transfer by convection at a cruising altitude of 12.2 km (18.8 kPa) for wide-body aircraft. These thermal challenges are exacerbated by implementing bipolar MVDC EPSs which are formed of two adjacent power cables, conventionally. In this regard, coaxial geometry for cables can be evaluated as a solution to this problem. In this paper, a coaxial MVDC power cable is, for the first time, designed with inner and outer conductors carrying the same ampacity of 1000 A when the voltage of the inner and outer conductors is -5 kV and +5 kV, respectively. This design compares the effectiveness of coaxial power cables to the conventional arrangement of bipolar MVDC cable systems. This study will analyze three case studies to determine if a coaxial geometry is better than a conventional arrangement for a bipolar MVDC cable system or not. According to the findings of this study, coaxial cable requires thicker insulation and more conductors to maintain the same maximum electric field norm within cable insulation and ampacity. As a result, coaxial cables result in a greater mass and cross-sectional area than standard bipolar cables. For the envisaged AEA, the investigation in this paper addresses questions about the performance of coaxial geometry for bipolar MVDC power cables.**

I. Introduction

In the United States, the transportation industry was responsible for the highest proportion (28%) of greenhouse gas (GHG) emissions in 2021 [1]. The implementation of all-electric transportation is considered a viable strategy for attaining the goal of achieving net-zero emissions by the year 2050. Although electric vehicles are at their maturity, the aviation industry is still in its early stages of electrification for commercial aircraft. Numerous recent studies have focused on implementing electrical systems in commercial aircraft as a replacement for traditional mechanical, hydraulic, and pneumatic systems. To meet the requirements of future generations of electrified aircraft, such as more electric aircraft (MEA) and all-electric aircraft (AEA), their electric power systems (EPS) which is an islanded microgrid [2] will need to be able to deliver a high amount of power while maintaining a low overall system mass [3]. As one of the main components of EPS, power cables show considerable potential for optimizing to attain a low-system-mass EPS. One potential approach to reduce the weight of cables and, consequently, the overall mass of the aircraft's electrical power system (EPS) is to implement higher voltage operations. In our previous studies, three bipolar ±5 kVdc EPS designs were discussed for a large-scale AEA [4] where a high ampacity of 1 kA is needed for the cables distributing the huge thrust power in three EPS designs.

Aviation power cables face various challenges, including partial discharge (PD), arc and arc tracking, surface charges, and thermal management. Among these challenges, thermal characteristics of a cable are crucial due to their significant influence on the cable's weight, dimensions, and maximum current capacity of the cable. At an altitude of 12.2 km (18.8 kPa), which is the cruising altitude for widebody aircraft, the heat transfer by convection is greatly reduced, resulting in a reduction of the maximum current flowing through the conductor [5-8]. Because bipolar MVDC power cables typically consist of two power cables adjacent to one another, these challenges are significantly more difficult since the goal is to reduce the volume of the cable ducts as well.

Using coaxial cable systems may decrease the total size/volume and weight of the aircraft's EPSs in bipolar MVDC systems. The authors in [9] developed a 23 kV/60 MVA coaxial HTS (High-Temperature Superconducting) power cable for a three-phase system. As a coolant, liquid nitrogen was used. In another work, an optimized 10 kV/1.5 kA three-phase coaxial HTS cable was designed for urban areas [10]. However, for low-pressure environments, a ±5 kV bipolar MVDC coaxial power cable that does not use active cooling methods has not been developed yet. This paper will address its viability as a potential replacement for the conventional arrangement of bipolar MVDC cable systems when the coaxial MVDC power cable is exposed to a low-pressure environment.

In this research, a new type of coaxial power cable with inner and outer conductors carrying the same ampacity of 1000 A is studied when the voltage of the inner and outer conductors are -5 kV and +5 kV, respectively. An elaborated coupled electric, thermal, and computational fluid dynamics (CFD) model is developed in COMSOL Multiphysics to optimally design the bipolar MVDC coaxial power cable with the rating targeted in this paper capable of operating at a low pressure of 18.8 kPa. Using the model, three case studies are examined to determine whether a coaxial design can be more effective than a traditional arrangement for envisaged aircraft bipolar MVDC cables.

II. Model

In this study, a comprehensive coupled electrical, thermal, and CFD model is developed in COMSOL Multiphysics to determine the distributions of the electric field and temperature field across the cables. The coupled physics in the model contains heat transfer, electric fields, electric currents, laminar flow, and surface-to-surface heat radiation modules. All heat transfer types including conduction, convection, and radiation are considered. In addition, the 5 kV MVDC NL-EPR cable configuration from Southwire is utilized in this investigation [11]. Fig. 1 shows the geometry of the conventional bipolar MVDC cable system containing two Southwire cables. The conventional cable's geometrical properties and the material properties of the cables used in the bipolar cable system are presented in Table I and Table II, respectively.

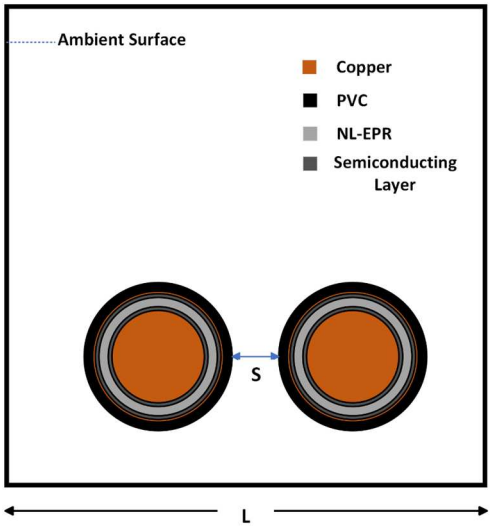

Fig. 1. The geometry of the conventional bipolar MVDC cable system considered in modeling and simulations.

TABLE I
Geometrical Characteristics of the Conventional Cable [11]

Parameters	Value
Conductor Diameter (mm)	28.372
Semiconductor Layer 1 Overall Diameter (mm)	29.769
NL-EPR Insulator Overall Diameter (mm)	34.341
Semiconductor Layer 2 Overall Diameter (mm)	35.865
Copper Layer Overall Diameter (mm)	36.119
PVC Jacket Overall Diameter (mm)	40.437
Maximum permissible temperature for normal condition (°C)	105

TABLE II
Thermal Properties of the Material of Cables

Parameters	NL-EPR	PVC	Semiconductor
Thermal Conductivity (W.(m.K)$^{-1}$)	0.3	0.19	10
Heat Capacity (J.(kg.K)$^{-1}$)	1800	1050	2405
Density (kg.m^{-3})	860	1350	1055
Surface Emissivity	-	0.91	-

The continuous operating temperature of the cable is up to 105°C. This temperature is used to calculate the maximum permissible current of the cables. For modeling heat radiation, the duct, shown as Ambient Surface in Fig. 1, is assumed to encapsulate the cables. The duct is a square-shaped domain with a 1 mm thickness. In our study, the size of the square-shaped duct, L shown in Fig. 1, is 250 mm. The outside of the duct has the same temperature as the ambient temperature, and the inner walls of the duct are in contact with the air domain inside the duct. S, shown in Fig. 1, is considered the distance between the negative and positive poles. Cables are mounted on post insulators 1 inch from the duct floor.

The coaxial geometry is compared with traditional geometry shown in Fig. 1 in three cases. In the first case, a coaxial cable with inner and outer copper conductors and a thicker NL-EPR insulation between inner and outer conductors is designed to have the same maximum electric field norm as a traditional bipolar cable system. Other layers, such as the semiconducting layer and the PVC jacket, have the same thickness as before. These thicknesses are independent of the diameter of the inner and outer conductors. The geometry of the coaxial cable (case I) is shown in Fig. 2. The cross-sectional area and mass of both inner and outer conductors are identical for this case.

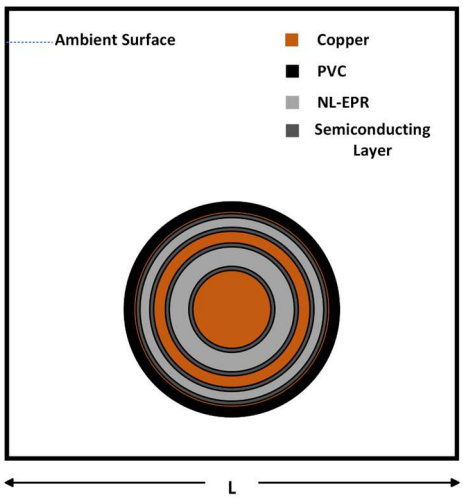

Fig. 2. The geometry considered for the coaxial cable system in case I.

For the second case (case II), a hollow area in the center of the inner conductor is considered to increase the surface area of the coaxial cable. Increasing the surface area of the coaxial cable yields higher radiative and convective heat transfers, thus at a constant ampacity, the cross-sectional area of the conductors can be decreased. In this case, the main concern is to calculate the total weight of the coaxial cable at different diameters of the hollow part when the cable's ampacity is considered as 1140 A. The current of 1140 A is the maximum permissible current of the conventional arrangement shown in Fig. 1 when there is a sufficient distance, S, between poles, obtained from the model. The geometry of the hollow coaxial cable is depicted in Fig. 3, where D_h is the diameter of the hollow area. To have the same cross-sectional area for both conductors, one can deduct that:

$$r_{con1}^2 - r_h^2 = r_{con2}^2 - r_{sm2}^2 \quad (1)$$

where r_{con1} is the radius of the outer part of the inner conductor, r_h is the radius of the hollow part, r_{con2} is the radius of the outer part of the outer conductor and r_{sm2} is the radius of the second semiconducting layer.

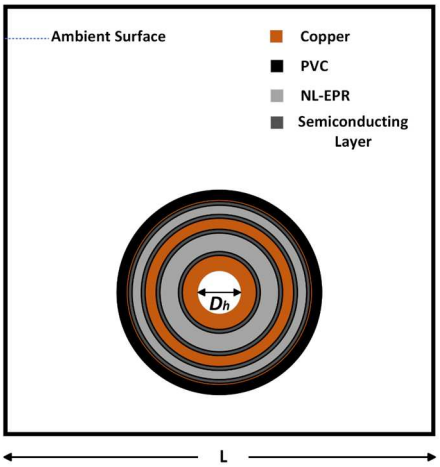

Fig. 3. The geometry considered for the coaxial cable system in case II.

In the third case (case III), the dimensions of the duct were modified to reach a maximum of 1-inch clearance from all sides of the duct for both coaxial and conventional arrangements. The configuration of the cables is identical to that of case 1, only the size of the ducts is reduced. For all three cases, the ambient temperature and pressure are 18.8 kPa and 40°C, respectively.

The heat is transferred via the insulating layers, conductors, and PVC jackets. From the cable's inner conductor to its outer jacket, the heat equation is as follows:

$$\rho C_p \frac{\partial T}{\partial t} + \nabla.(-k\nabla T) = Q + q_o \tag{2}$$

where ρ is the density (kg.m^{-3}), T is the temperature (K), k is thermal conductivity (W.(K.m)$^{-1}$), q_o is the heat flux (W.m^{-3}), and C_P is the specific heat capacity at constant pressure (J.(kg.K)$^{-1}$). The total amount of radiation emitted and absorbed by the cable and duct can be calculated as

$$q_{12} = \varepsilon_{eq}\sigma_S(T_S^4 - T_{amb}^4) \tag{3}$$

where σ_S is Stefan's constant (W/(m^{2}K^4), T_s and T_{amb} are temperature (K) of the surface of cable and the ambient temperature, respectively, and ε_{eq} is equal emissivity and is expressed as

$$\varepsilon_{eq} = \frac{A_1}{\frac{1-\varepsilon_1}{\varepsilon_1} + \frac{1}{F_{12}} + \frac{1-\varepsilon_2}{\varepsilon_2\left(\frac{A_2}{A_1}\right)}} \tag{4}$$

where A_1 and A_2 are the cable surface and ambient surface area, respectively, ε_1 and ε_2 are the surface emissivity, and F_{12} is the view factor represented as

$$F_{12} = \frac{1}{A_1}\int_{A_1}\int_{A_2} \frac{cos\theta_1 cos\theta_2}{\pi R^2} dA_1 dA_2 \tag{5}$$

where dA_1 and dA_2 are elemental areas, R is the linking line between the surfaces, θ_1 and θ_2 are polar angles created by R and surface normal. Also, natural heat convection is responsible for transferring heat in the air domain.

The DC conductivity of polymers can typically be expressed by empirical formulas such as:

$$\sigma(E,T) = Aexp\left(\frac{-\varphi q_e}{k_b T}\right)\frac{\sinh(B(T)\ln(E))}{E^\gamma} \tag{6}$$

where q_e is the electron charge, k_b is Boltzmann's constant, E is the electric field (V.m^{-1}), φ is the thermal activation energy, σ_0, A and γ are constants, and $B(T)$ is a parameter that depends on the temperature. The electric field distribution is calculated by

$$E = -\nabla V \tag{7}$$

$$J_e = \sigma E \tag{8}$$

where V is the voltage (V), J_e is the current density (A.m^{-2}), and σ is the conductivity (S.m^{-1}). The temperature, velocity, and electric fields are coupled, as shown by Eqs. (2)–(8). The study time is determined to be 30 hours to reach the steady case.

III. Simulation Results

The primary goal of this study is to evaluate the performance of the coaxial geometry in comparison to the traditional arrangement of bipolar MVDC power cables operating under low pressures. For this, three aforementioned cases are considered. All of those cables were designed to have the same maximum electric field in their insulation, E_{max}, meaning they were designed to experience the same maximum electric stress condition. To this end, the insulation thickness of the coaxial cable's inner insulator, between inner and outer conductors, must be approximately two times of those conventional separate poles shown in Fig. 1. The thickness of the outer insulator can be identical to that of a single pole cable in Fig. 1.

A. Case I: Coaxial Cable with the Same Cross-Sectional Area

In Case I, both inner and outer conductors of the coaxial cable have the same cross-sectional area and each corresponds to one pole in the configuration shown in Fig. 1. For the arrangement shown in Fig. 1, by changing S, the maximum permissible current increases to reach a constant value. The Maximum permissible current at different amounts of S and the coaxial cable of Case I are presented in Table III.

TABLE III
Maximum Permissible Current of the Cables (Case-I)

Cable types	Max. Permissible Current (A)
Bipolar (S=0 inch)	1045
Bipolar (S=1 inch)	1140
Bipolar (S=2 inch)	1140
Coaxial Cable	990

990 A is the maximum current permissible for the coaxial cable, compared to 1045 A, 1140 A, and 1140 A for the conventional arrangement with S=0, 1, and 2 inches.

B. Case II: Coaxial Cable with a Hollow Conductor

Increasing the total diameter of the coaxial geometry results in larger radiative and convective heat transfers, and in turn, larger maximum permissible current. To this end, the inner conductor can be considered a hollow conductor as shown in Fig. 3. In this regard, for a given ampacity, the cross-sectional area of the coaxial cable can be decreased by increasing the diameter of the hollow area. To determine the total weight of the coaxial cable at various diameters of the hollow part, the

cable's ampacity is fixed as 1140 A, calculated above, which is the maximum permissible current of the conventional arrangement. The weight per meter (kg/m) of the cable with different diameters of the hollow part is shown in Fig. 4 when the coaxial cable's ampacity is 1140 A.

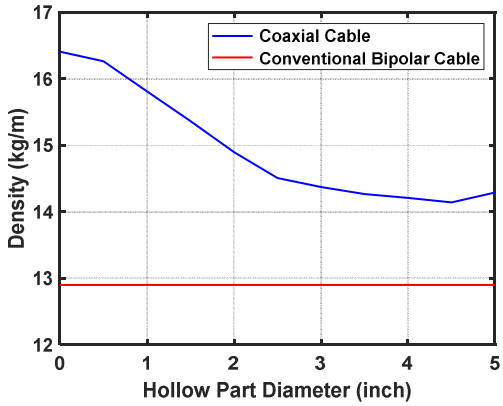

Fig.4. The weight per meter (kg/m) of coaxial cable with different hollow part diameters, Case II.

The results show that by increasing the diameter of the hollow part, the weight of the cable reduces to a point and then increases, since the thickness of the insulations, semiconducting layers, and jacket remains constant. The maximum weight per length is 16.409 kg/m for no hollow part. The minimum weight is 14.142 kg/m for a hollow part's diameter of 4.5 inches, which is higher than the sum of the conventional bipolar cable's weight, 12.99 kg/m. For larger hollow parts than 4.5 inches, the total weight of the coaxial cable increases.

C. Case III: Coaxial Cable in a Smaller Duct

For both coaxial cable without a hollow part and the conventional bipolar cable system at S=0, the distance of the cables from all sides of the duct was reduced to 1 inch. The results show that, for Case III, at 18.8 kPa, the maximum permissible current of the coaxial cable is less than that of the conventional bipolar system. It is worth mentioning that the surface area of the duct for the coaxial cable is larger than the conventional bipolar system, e.g., 18.62 inch^2 compared to 19.57 inch^2. In another study, Case III was conducted at the pressure of 1 atm. Although at the pressure of 1 atm, the difference between the maximum permissible current of the coaxial cable and the conventional arrangement reduces compared to the pressure of 18.8 kPa, the maximum permissible current of the coaxial cable is still smaller than that of the conventional arrangement shown in Fig. 1 even at S=0.

In our other studies, a cuboid geometry design was studied in [12, 13] while the influence of vertical and horizontal arrangements of a conventional bipolar cable on the maximum permissible current of the cable was studied in [14]. Note the horizontal arrangement shown in Fig. 1 can also be considered to be vertical which as mentioned above was studied in [14].

IV. Conclusion

In this paper, for the first time, a coaxial geometry for a bipolar MVDC power cable envisaged for all electric wide-body aircraft is designed and compared with the conventional arrangement/geometry, to see whether the coaxial design shows a higher maximum permissible current or smaller weight and size than the conventional arrangements. Three case studies have been conducted to compare different coaxial designs a conventional one. For the first case, with the same cross-sectional area for the coaxial and conventional designs, the maximum permissible current of the coaxial cable is lower than the conventional one. For the second case, with the same ampacity of 1140 A, the designed coaxial cable weighed more than the conventional one. For the third case with a smaller duct size, despite the fact that the duct surface area is increased for the coaxial design, the maximum permissible current of the coaxial cable is still lower than the conventional one.

Acknowledgment

This work was supported in part by the U.S. Advanced Research Projects Agency-Energy (ARPA-E) under Award DE-AR0001677, in part by the U.S. National Science Foundation (NSF) under Award 2306093, and in part by the U.S. Air Force Office of Scientific Research under Award FA9550-20-1-033.

References

[1] "Sources of Greenhouse Gas Emissions," *EPA*. [Online]. Available: https://www.epa.gov/ghgemissions/sources-greenhouse-gas-emissions.

[2] M. Hamidieh and M. Ghassemi, "Microgrids and resilience: A review, " *IEEE Access*, vol. 10, pp. 106059–106080, Oct. 2022.

[3] A. Barzkar and M. Ghassemi, "Components of electrical power systems in more and all-electric aircraft: A review," *IEEE Trans. on Transp. Electrific.*, vol. 8, no. 4, pp. 4037–4053, Dec. 2022.

[4] M. Ghassemi, A. Barzkar, and M. Saghafi, "All-electric NASA N3-X aircraft electric power systems," *IEEE Trans. Transp. Electrific.*, vol. 8, no. 4, pp. 4091–4104, 2022.

[5] A. Azizi, M. Ghassemi, and J. M. Lehr, "Heat transfer challenges for MVDC power cables used in wide body all electric aircraft under low pressures," *IEEE Access*, vol. 10, pp. 111811–111819, 2022.

[6] A. Azizi, M. Ghassemi, and J. Lehr, "Influence of low pressure on thermal limit of MVDC power cables used in all electric aircraft," *IEEE Int. Power Modulator and High Voltage Conf. (IPMHVC)*, 2022, pp. 88–91.

[7] A. Azizi, M. Ghassemi, and J. Lehr, "Design of a cable system for a high-power density MVDC aircraft electric power system," *IEEE Conf. Elect. Insul. Dielectr. Phenomena (CEIDP)*, 2022, pp. 151–154.

[8] A. Azizi and M. Ghassemi, "Design of high power density MVDC cables for wide body all electric aircraft," *IEEE Trans. Dielectr. Electr. Insul.*, Early Access, 2023, doi: 10.1109/TDEI.2023.3285849.

[9] S. J. Lee and H. S. Yang, "Recent progress and design of three-phase coaxial HTS power cable in Korea," *IEEE Trans. Appl. Supercond.*, vol. 29, no. 5, pp. 1–5, 2019.

[10] Q. Yang *et al*., "Optimization of a three-phase coaxial 10 kV/1.5 kA HTS power cable for balancing 3-phase current distribution," *IEEE Trans. Appl. Supercond.*, vol. 32, no. 6, pp. 1–5, 2022.

[11] "1/c CU 5kv 90 NLEPR 100% PVC MV-105," Southwire, https://www.southwire.com/wire-cable/medium-voltage-power-cable/1-c-cu-5kv-90-nlepr-100-pvc-mv-105/p/MV20 (accessed May 30, 2023).

[12] A. Azizi, A. Saha, and M. Ghassemi, "A cuboid geometry design for MVDC power cables for using in future all electric wide body aircraft," *IEEE Conf. Electr. Insul. Dielectr. Phenomena (CEIDP)*, 2023.

[13] A. Saha, A. Azizi, and M. Ghassemi, "Optimal bipolar MVDC power cable designs for future wide-body all electric aircraft," *IEEE Trans. Dielectr. Electr. Insul.*, submitted for publication.

[14] A. Azizi and M. Ghassemi, "A FEM coupled electrical, thermal, and computational fluid dynamic model and a theoretical Model for calculation of maximum permissible current in envisaged wide-body all-electric aircraft bipolar MVDC power cables," *IEEE Trans. Dielectr. Electr. Insul.*, submitted for publication.